Acta Polytechnica **53**(Supplement):612–616, 2013
doi:10.14311/AP.2013.53.0612

available online at http://ojs.cvut.cz/ojs/index.php/ap

GALACTIC AND EXTRAGALACTIC SUPERNOVA REMNANTS AS SITES OF PARTICLE ACCELERATION

Manami Sasaki*

Institute for Astronomy and Astrophysics, University of Tübingen, Germany

* corresponding author: sasaki@astro.uni-tuebingen.de

Abstract. Supernova remnants, owing to their strong shock waves, are likely sources of Galactic cosmic rays. Studies of supernova remnants in X-rays and gamma rays provide us with new insights into the acceleration of particles to high energies. This paper reviews the basic physics of supernova remnant shocks and associated particle acceleration and radiation processes. In addition, the study of supernova remnant populations in nearby galaxies and the implications for Galactic cosmic ray distribution are discussed.

Keywords: supernova remnants, shock waves, cosmic rays.

1. Introduction

Supernova remnants (SNR) are among the most beautiful astronomical objects, presenting various kinds of morphologies. At the same time they are important astrophysical sites, being responsible for the chemical enrichment, the energy budget, and the dynamics in the interstellar medium (ISM), and thus they drive the chemical and dynamical evolution of galaxies. In the optical, SNRs were identified as nebulae formed at the sites of historical supernovae (SNe). Most of the SNRs in our Galaxy were discovered as non-thermal, extended radio sources with a flux spectrum described by a power-law $S_\nu \propto \nu^\alpha$ with $\alpha \approx -0.5$. This emission was explained as synchrotron radiation emitted by a non-thermal, power-law population of relativistic electrons with $N(E) = KE^{-s}$ electrons cm^{-3} erg^{-1}. These electrons produce a power-law photon distribution with $\alpha = (1-s)/2$, thus $s = 2$ for $\alpha = -0.5$.

2. SNRs as a cosmic particle accelerator

Electrons that emit radio synchrotron emission observed in radio SNRs typically have energies in the GeV range. Particles of such energies and higher are known as cosmic rays (CRs). Since the first detection of CRs on the earth, many observations have been performed to study their nature and have shown that the all-particle spectrum of CRs can be described by a power-law $\propto E^{-2.7}$ up to $\sim 3\times10^{15}$ eV (the *knee*) and becomes steeper for higher energies. In general, CRs up to the *knee* are believed to be of Galactic origin, while extragalactic sources are discussed for CRs at higher energies.

Fermi [1] had suggested back in 1949 that particles can be accelerated in a diffusive process through magnetic mirroring of charged particles at moving magnetized interstellar clouds. Likely sites of particle accelerations in the interstellar space are the strong shock waves in SNRs, which are the remains of supernova explosions and heat the ambient ISM and distribute heavy elements that were processed inside the progenitor star throughout the Galaxy. These blast waves of shell-type SNRs have kinetic energy of the order of 10^{51} erg. The rate at which SNe occur in our Galaxy is estimated to be about 3 SNe per century, while each of these events can convert $\sim 10\,\%$ of their kinetic energy into cosmic-ray energy. SNRs are thus believed to be the primary sources of cosmic rays below 3×10^{15} eV (e.g., [2]).

2.1. Evolution of SNRs

After the initial explosion, SNRs go through the following evolutionary stages:

(1.) The ejecta dominated, free expansion phase in the first hundreds of years, in which the mass of the supernova ejecta, $M_{\rm ej}$, dominates over the mass of the swept up ISM.

(2.) The Sedov–Taylor phase or the *adiabatic* phase, in which $M_{\rm sw} > M_{\rm ej}$. The radiative losses are still negligible. In this phase, which typically lasts a few 1000–10,000 yr, the SNR expands adiabatically.

(3.) In the subsequent pressure-driven or *snow-plough* phase, radiative cooling becomes dynamically important. The evolution of the shock radius is best described by using momentum conservation.

(4.) Finally, in the merging phase the shock velocity and the temperature behind the shock become comparable to the turbulent velocity and temperature of the ISM, respectively. The SNR becomes fainter and fainter and merges with the ISM.

Figure 1 (left) shows a three-colour X-ray composite image of Tycho's SNR, which is 440 years old and is believed to be in the transition between the free expansion phase and the Sedov phase. The outer blast wave is well seen in hard X-rays (blue/violet), while

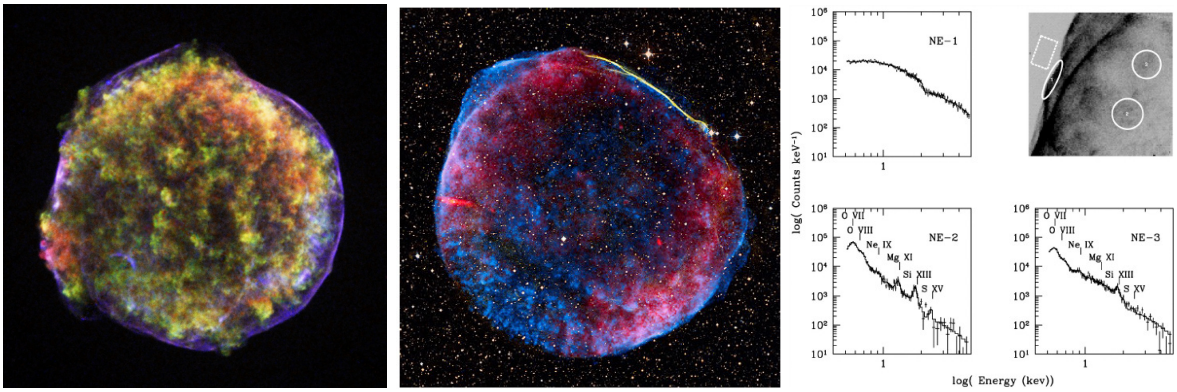

FIGURE 1. *Left:* Tycho's SNR observed with the *Chandra X-ray Observatory*. The image is a composite of three X-ray images at the following energies: $0.95 \div 1.26$ keV (red), $1.63 \div 2.26$ keV (green), $4.1 \div 6.1$ keV (blue). (NASA/CXC/Rutgers/J. Warren & J. Hughes et al.) *Middle:* Composite image of the remnant of SN 1006 consisting of X-ray data from *Chandra* in blue, optical data from the University of Michigan's 0.9 m Curtis Schmidt telescope at the Cerro Tololo Inter-American Observatory (yellow) and the Digitized Sky Survey (orange and light blue), and radio data from the Very Large Array and Green Bank Telescope in red. (X-ray: NASA/CXC/Rutgers/G. Cassam-Chenaï, J. Hughes et al.; Radio: NRAO/AUI/NSF/GBT/VLA/Dyer, Maddalena, & Cornwell; Optical: Middlebury College/F. Winkler, NOAO/AURA/NSF/CTIO Schmidt & DSS). *Right: Chandra* spectra of the outer rim (1) and two interior regions (2, 3) of the northeastern limb of SN 1006 by Long et al. [7]. While the spectrum of the outermost region is a simple power-law, the spectra of inner region are have significant thermal components.

the interior red-greenish, softer X-ray emission is due to hot ejecta.

2.2. Shock waves in SNRs

The strong expansion due to supernovae form waves in the surrounding medium with high-amplitude disturbances resulting in a discontinuous flow. Discontinuities of velocity v, pressure p, and density ρ in non-stationary flows are produced by shock waves. In the rest frame of the shock front, the gas moves perpendicular to the shock from side 1 (upstream) to side 2 (downstream). In reality the shock front propagates into region 1. At the shock front, the conservation laws of mass, energy, and momentum flow must be fulfilled. For a monoatomic gas, the ratio of the specific heats is $\gamma = 5/3$. For a Mach number M with $M^2 \gg 1$, one obtains $r = \rho_2/\rho_1 = u_1/u_2 = \frac{\gamma+1}{\gamma-1} = 4$ and $kT_2 = \frac{3}{16}\mu_2 m_p u_1^2$, where μ is the mean mass per particle ($\mu_2 \approx 0.6$ for fully ionized gas of cosmic composition downstream). Upstream, μ_1 may be 1.4 in the case of a (mostly diatomic) neutral gas of cosmic composition.

However, these relations are correct only if the energy loss due to radiation or other causes is negligible. If efficient acceleration of particles in shocks occurs, the energy loss due to escaping particles can become significant. In addition, a relativistic particle population will lower the mean adiabatic index from 5/3 to its fully relativistic value of 4/3.

The primary mechanism discussed for producing energetic particles in SNR shocks is diffusive shock acceleration (DSA, [3–5], etc.). In a collisionless shock wave like in an SNR, the velocities of particles are randomized by scattering at inhomogeneities in the magnetic field. A considerable fraction of the particles may scatter back upstream, hence particles can cross the shock front many times and gain energy. Owing to these processes, the energy distribution of the particles develops a non-thermal power-law tail in addition to a Maxwellian distribution. Particles accelerated in SNR shocks will also have a dynamical effect on the shock. The incoming gas (in the shock frame) will be decelerated as accelerated particles diffuse ahead and scatter at inhomogeneities in the magnetic field in the upstream medium. Therefore, the upstream flow is gradually slowed by the accelerated particles. The thermal shock in which the gas is heated still persists. In total, the compression ratio becomes larger than in the DSA-free case. Particles with higher energies will get farther ahead of the shock front, where the compression ratio is higher. This will result in a harder spectrum and a concave up-curvature in the particle spectrum is expected. In addition, accelerated particles, which get ahead of the shock, can themselves excite magnetohydrodynamic waves [6]. The interstellar magnetic field thus can be amplified at the shock of young SNRs through these self-generated magnetohydrodynamic waves, which can again scatter particles.

2.3. Observations of SNRs

Reynolds & Chevalier [8] first proposed that DSA might cause X-ray synchrotron emission in SN 1006, in which predominantly non-thermal emission was detected (Fig. 1, middle and right). In addition, two synchrotron-dominated shell-type X-ray SNRs were discovered in the 1990s: RX J1713.7-3946 (G347.3-0.5, [9, 10]) and Vela Jr. (G266.2-1.2, [11, 12]). Synchrotron emitting thin filaments were also found in remnants of historical SNe RCW 86 (SN 185), Tycho (SN 1572), Kepler (SN 1604), or Cas A (SN ∼1667).

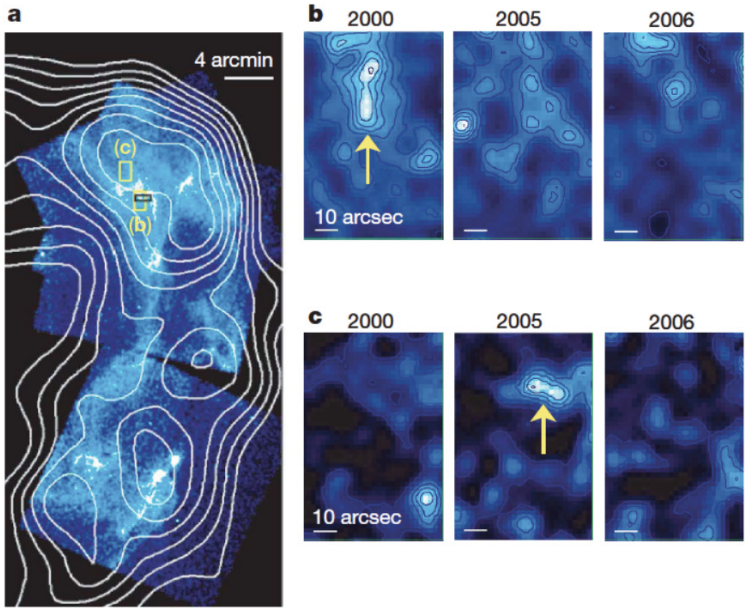

Figure 2. *Chandra* image of SNR RX J1713.7–3946 with H.E.S.S. contours [13].

2.3.1. Magnetic field in the non-thermal filaments

As the synchrotron flux depends on the magnetic field strength, the non-thermal filaments observed in X-rays can be used to derive the magnetic flux density B. The very thin synchrotron filaments found in X-rays parallel to the remnant edge indicate a fast drop of synchrotron emissivity behind the shock, which is far too fast to be explained by adiabatic expansion of electrons and the magnetic field. Therefore, either the X-ray emitting electrons must disappear through radiative losses or the magnetic field must decay through some damping mechanisms. If electron losses are the cause, the filament width corresponds to the distance that electrons convect in the post-shock flow within synchrotron loss time. Typical filament thicknesses of ~ 0.01 pc imply immediate post-shock magnetic field strengths between 50 and 200 µG for the historical SNRs.

Non-thermal X-ray hot spots were found in SNR RX J1713.7–3946, which brightened and decayed on a one-year timescale (Fig. 2, [13]). The rapid variability of the X-ray hot spots shows that the acceleration of the ultrarelativistic synchrotron-emitting electrons is associated with an amplification of the magnetic field by a factor of more than 100.

2.3.2. Supernova remants interacting with molecular clouds

Another scenario in which the acceleration of particles results in traceable emission at or around SNRs is the acceleration of heavier particles, which then interact with the ambient dense gas and produce pions through inelastic scattering on thermal protons. The neutral pion π^0 decays to gamma rays, which produce a spectrum peaking at energy $m_\pi/2 = 68$ MeV and continuing to higher energies with the same shape as the primary ion spectrum.

SNRs located in an inhomogenous ISM and interacting with molecular clouds like SNRs IC 443, W28, W51C are likely sources of π^0-decay emission. At the position of these SNRs, CO clouds or OH masers have been found, which indicate that the SNR shock wave is interacting with some high-density medium (Fig. 3).

3. Studies of extragalactic SNRs

Supernova remnants can best be studied in soft X-rays, since they mainly consist of very hot plasma ($10^6 \div 10^7$ K) and radiate copious thermal line and continuum emission. However, due to absorption by interstellar matter, it is often difficult to study these soft X-ray sources with predominant emission below 10 keV in our own Galaxy.

3.1. SNR 1E 0102.2–7219 in the Small Magellanic Cloud

SNR 1E 0102.2–7219 is the brightest X-ray SNR in the Small Magellanic Cloud (SMC), which shows strong line emission of highly ionized O, Ne, and Mg. Optical filaments have also been detected with radial velocities of -2500 to $+4000$ km s^{-1} w.r.t. the SMC [16]. *Chandra* grating spectrum indicates velocities of ± 1000 km s^{-1} [17].

Hughes et al. [18] studied the *Chandra* data of SNR 1E 0102.2–7219 and concluded that the optical filaments and the extent measured from the *Chandra* images indicate a higher expansion velocity what would correspond to the post-shock electron temperature derived from the X-ray spectra. Even taking into account that the electrons and heavier particles in the shock have not reached thermal equilibrium, which thus corresponds to non-equilibrium ionization, is not

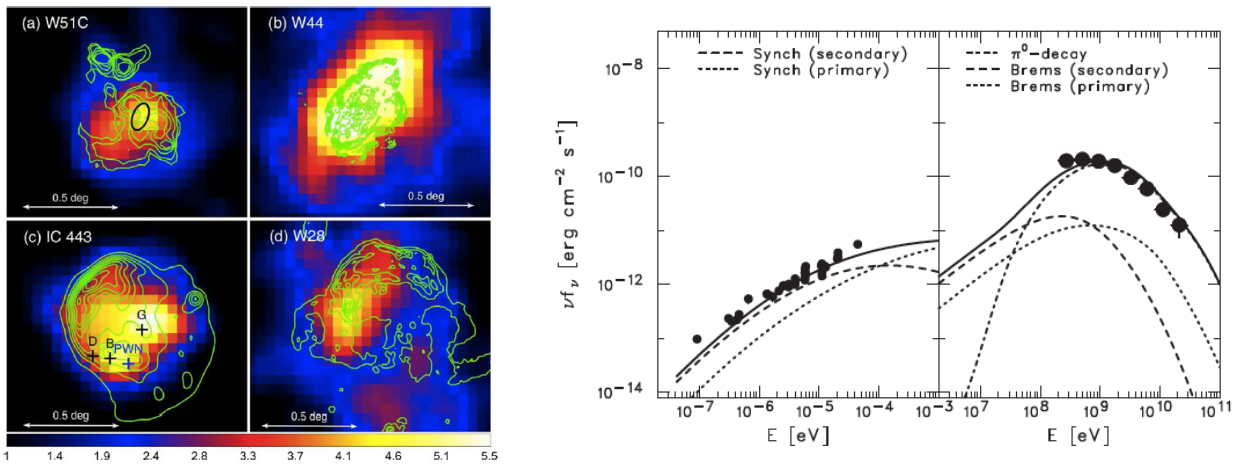

FIGURE 3. *Left:* Fermi LAT 2 – 10 GeV count maps with VLA radio contours (ellipse: shocked CO clump, crosses: OH masers, [14]). *Right:* Radio and γ-ray spectra of SNR W44 with models [15].

sufficient to yield the observed inconsistency. Therefore, the authors suggest that cosmic rays must have carried a significant fraction of the SNR shock energy away. Theoretial calculations have shown that non-linear effects in particle acceleration mechanisms can yield a mean post-shock temperature of ~ 1 keV for SNR 1E 0102.2–7219 [19, 20], consistent with the observed X-ray temperature, e.g., [18, 21].

3.2. SNRs in nearby galaxies

As supernova remnants are believed to be the primary sources of Galactic cosmic rays, the distribution of SNRs is essential for understanding the injection and propagation of Galactic cosmic rays. However, the galactic position of the Earth is not ideal for studying the source distribution in our Galaxy. To understand the distribution of SNRs in a spiral galaxy, it is necessary to study other nearby spiral galaxies.

We have obtained a new complete sample of X-ray SNRs in M 31 based on the *XMM-Newton* Large Programme survey data [22]. In Fig. 4 we compare the radial number distribution of X-ray SNRs in M 31 to that of Galactic SNRs and of X-ray SNRs in M 33 [23]. The SNR distributions in M 31 and M 33 are comparable but slightly flatter than in the Milky Way. The distribution of SNRs in M 31 is correlated with the distribution of gas in M 31, which shows ring-like structures with the most prominent ring at a radius of ~ 10 kpc. The flatter SNR distribution in M 33 is consistent with M 33 being a typical flocculent spiral galaxy with discontinuous spiral arms and prominent on-going star formation regions in these arms.

4. Summary

Supernova remnants are the aftermath of stellar explosions, which inject large amounts of energy into the ISM, carving out new structures and transferring kinetic energy to the ISM. In addition, particles can be accelerated in the SNR shock waves through diffusive shock acceleration. Rather recent GeV to TeV observations of SNRs have confirmed the existence of ultrarelativistic particles in SNRs.

The primary agent of the acceleration process are the magnetic fields, which can also be modified and amplified by the relativistic particles. Measurements of X-ray synchrotron emission in non-thermal SNRs allow us to derive the magnetic field and its configuration around the shock. The relativistic particles in the SNR shock also modify the shock itself by carrying away kinetic energy from the SNRs. In addition, SNRs interacting with dense molecular clouds are likely to produce γ-rays via π^0 production with subsequent decay.

While observations of Galactic SNRs emitting non-thermal X-ray emission or γ-rays help us to improve our understanding of CR acceleration in SNR shocks, observations of extragalactic SNRs allow us to perform statistical studies of a representative sample of the sources within a galaxy. The spatial distribution of SNRs in a galaxy will shed light on the propagation of cosmic rays in the galaxy.

References

[1] Fermi E., 1949, Phys. Rev. 75, 1169
[2] Hillas A.M., 2005, J. Phys. G: Nucl. Part. Phys. 31, R95
[3] Drury L.O'C., 1983, Rep. Progr. Phys. 46, 973
[4] Blandford R.D., Eichler D., 1987, Phys. Rep. 154, 1
[5] Jones F.C., Ellison D.C., 1991, Space Sci. Rev. 58, 259
[6] Bell A.R., 1978, MNRAS 182, 147
[7] Long, K.S., et al., 2003, Ap. J. 586, 1162
[8] Reynolds S.P., Chevalier R.A., 1981, Ap. J. 245, 912
[9] Koyama K., et al., 1997, Publ. Astron. Soc. Jpn. 49, L7
[10] Slane P., et al., 1999, Ap. J. 525, 357
[11] Aschenbach B., 1998, Nature 396, 141
[12] Slane P.O., et al., 2001, Ap. J. 548, 814
[13] Uchiyama Y., et al., 2007, Nature 449, 576
[14] Uchiyama Y. on behalf of the Fermi LAT collaboration, 2011, arXiv:1104.1197

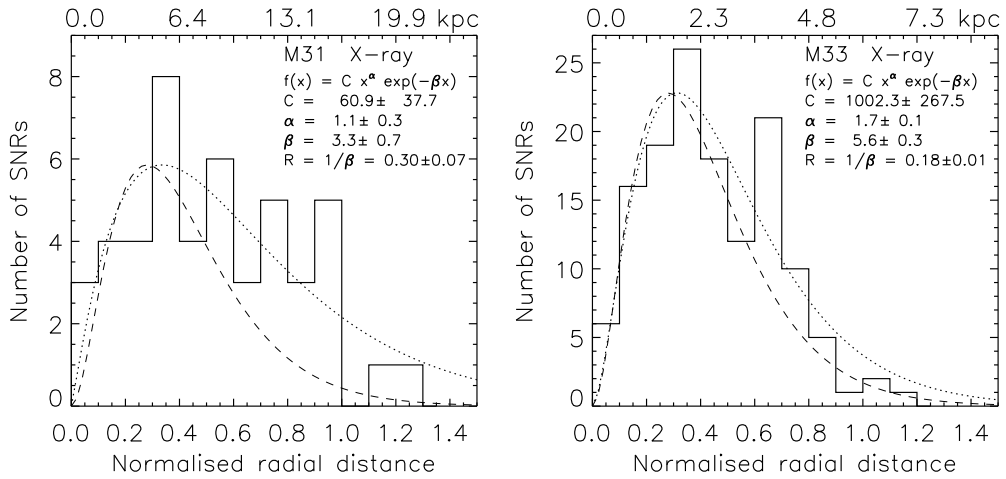

Figure 4. Surface density of SNRs and candidates in M 31 [22] and M 33 [23] plotted over the radius normalised to half of the apparent major isophotal diameter $D_{25}/2$. The radial distance in kpc is given along the upper x-axis. Dotted lines show the fitted model function $f(x) = Cx^{\alpha} \exp(-\beta x)$, dashed lines show the model function for the Milky Way [24] normalised to the maximum of M 31 or M 33.

[15] Thompson D.J., Baldini L., Uchiyama Y., 2012, arXiv:1201.0988

[16] Tuohy I.R., Dopita M.A., 1983, Ap. J. 268, L11

[17] Flanagan K.A., et al., 2004, Ap. J. 605, 230

[18] Hughes J.P., Rakowski C.E., Decourchelle A., 2000 Ap. J. 543, L61

[19] Decourchelle A., Ellison D.C., Ballet J., 2000, Ap. J. 543, L57

[20] Ellison D.C., 2000, AIP Conf. Proc. 528, 386

[21] Sasaki M., et al., 2006, Ap. J. 642, 260

[22] Sasaki M., et al., 2012, arXiv:1206.4789

[23] Long K.S., et al., 2010, Ap. J. S. 187, 495

[24] Case G.L., Bhattacharya D., 1998, Ap. J. 504, 761

Discussion

Carlotta Pittori's comment — I have a comment on the SNR W44. You just quoted γ-ray *Fermi* data. One of the most important recent AGILE results is about this SNR (Giuliani et al., 2011, ApJL, 742, 30). AGILE data extend to the lowest part of the γ-ray spectrum energy distribution around 100 MeV and allow us to discriminate between leptonic and hadronic models, providing the first clear evidence of π^0-decay and of proton acceleration.